

# Numerical Investigation of Heat Transfer on a Flat Plate with Pulsating Jet Array along with Cross Flow Assisted with Baffles

Issac John<sup>1</sup>, Sabu Kurian<sup>2</sup>

<sup>1</sup> Student, Dept. of Mechanical Engineering, M A College of Engineering, Kothamangalam, Kerala, India

<sup>2</sup> Associate Professor, Dept. of Mechanical Engineering, M A College of Engineering, Kothamangalam, Kerala, India

\*\*\*

**Abstract** – A numerical study based on jet impingement heat transfer was carried out by computational fluid dynamics in order to evaluate the effect of cross flow assisted with baffles on the pulsating jet impingement heat transfer. The study investigates the effect of pulsating jets for different baffle length along with variation in cross flow velocity. Additionally, the potential of the impinging jet in a cross-flow configuration was assessed. It was found that the baffle with 9mm gap showed the highest degree of average Nusselt number and temperature. The plate to nozzle plane distance was kept constant throughout the investigation. The frequency of the pulsation of jets was also kept constant.

**Key Words:** Baffles, Cross flow, Nusselt number, pulsating jet impingement

## 1. INTRODUCTION

Heat transfer is a normal process that takes place in day-to-day life. The process of heat transfer can be classified into three viz., conduction, convection and radiation. The process of transfer of heat by the bulk movement of fluid is called convection. It is an important mode of heat transfer in industries for various heating and cooling purposes, also in the cooling of automobile engines and electronics. The advancement in science had led to highly complicated electronic devices and at the same time the size of such devices is getting reduced day by day. The amount of heat generated by these devices is increasing in par with its complexity.

The efficiency of electronics devices decreases with increase in temperature. The cooling of these devices to their normal working temperature is a great challenge since the area available for heat transfer will be very less and there is restricted movement of air. Many new methods of cooling had been adopted to meet the cooling requirements of electronic devices.

Cooling of electronic devices is going to be the major challenge that will be faced by the electronic industry in the coming future. The demand for better heat transfer from smaller and smaller surfaces is increasing day by day with the exponential growth of electronic industry. Many researchers have come up with different technologies for the cooling challenge throughout recent years, among which cooling with a high velocity fluid jet directly impinging on heat transfer surface become a promising

heat transfer method to meet the needs of electronic industry. In this study we focus on pulsating jet impingement heat transfer, along with cross flow assisted with baffles.

In the literature, we note that the majority of works which were interested in this problem are experimental. Womac D and Incropera (1), investigated experimentally on steady air jets and have shown that higher heat transfer coefficients result from submerged jet conditions than from free-surface jet conditions for  $Re \geq 4000$ . They also found that the presence of a confining top wall in jet impingement causes lower heat transfer coefficients, thought to be caused by the recirculation of fluid heated by the target plate. Dushyant Singh, B. Premachandran(2), carried out A detailed parametric study was experimentally to understand the effects of  $Re$ ,  $h/d$  and  $d/D$  on local Nusselt number distribution. It was observed that the stagnation Nusselt number increases monotonically as the  $h/d$  decreases and the effects of  $h/d$  and  $d/D$  are significant only in the jet impinging region. Heat transfer rate was higher at lower  $h/d$  ratios. Stagnation Nusselt number always decreases on increasing  $h/d$  ratios.

Jung -Yang San(3), experimentally investigated the effect of jet to jet spacing on local Nusselt number for circular air jets vertically impinging on a flat plate. Five jets in equilaterally staggered arrays were considered. The influence of jet to jet spacing,  $Re$  and jet height on stagnation Nusselt number of the centre jet was investigated. For smaller jet spacing due to shear layer expansion interference between two adjacent jets will occur. It weakens jet strength and eventually degrade the heat transfer. For different Reynolds number (10,000-20,000), got optimum  $S/d$  (4-16) for different  $H/d$  (2,3, 5) values.

R. Zulkifli, K. Sopian(4), conducted an experimental study on pulsejet impingement heat transfer. Pulsation of the air jet was produced by a rotating cylinder valve mechanism at frequencies between 10 to 80 Hz. A heated circular pulsating air jet at different pulse frequencies and Reynolds Number was used to measure the average and local heat flux on the impingement plate. Results obtained show that the local Nusselt number calculated were higher at all radial position away from the stagnation point. The pulsed jet Nusselt number was higher than the average

steady jet Nusselt number for all values of frequencies due to the higher localized heat transfer. The higher Nusselt number obtained at localized radial positions can be due to the higher instantaneous velocity. Enhanced turbulence intensity found was due to the pulsed jet. Angioletti (5), extensively investigated the flow field behavior in the vicinity of the stagnation region. Later, by using commercial CFD package, they evaluated the suitability of three different turbulence models by comparing the numerical results with the experimentally obtained results. They found that the  $k-\omega$  SST (shear stress transport) model gave good result for lower Re and  $k-\epsilon$  RNG (renormalization group) or RSM (Reynolds stress model) performed better for high Re.

Gorka S. Larraona (6), conducted a parametric study based on design of experiments (DoE) techniques was carried out by computational simulation in order to evaluate the effect that design parameters have on heat transfer and pressure loss of an impinging jet in a cross-flow configuration. The main effects of each parameter and the interactions between parameters were analyzed in detail through the Response Surface Methodology (RSM). Additionally, the potential of the impinging jet in a cross-flow configuration was assessed by calculating the optimal values of the parameters and comparing the cooling efficiency of the resulting configuration with the efficiency of the conventional cross-flow configuration.

Many investigations on heat transfer characteristics of jet impingement cooling had been conducted; however no analysis have been done for pulsating jet impingement along with cross flow assisted with baffles. The current numerical study aims to analyze the heat transfer effect flat plate using pulsating air jets with cross flow assisted with baffles.

## 2. NUMERICAL MODEL

### 2.1 Geometry

The geometric model was drawn using the commercial software Ansys Fluent 16.2. It is shown in fig.1. Total there were 5 number of nozzles arranged in a staggered way. All nozzles were of same diameter and placed at a same distance from each other. All nozzles were at the same distance from the plate surface and they were allowed to start at the same time. The cross flow attacks the flow field from right side and exits through the left side. Baffles were arranged equidistant to each other on alternate sides of the flow field. The cross flow velocity and the gap between baffle and the impinging plate was varied to study different cases.

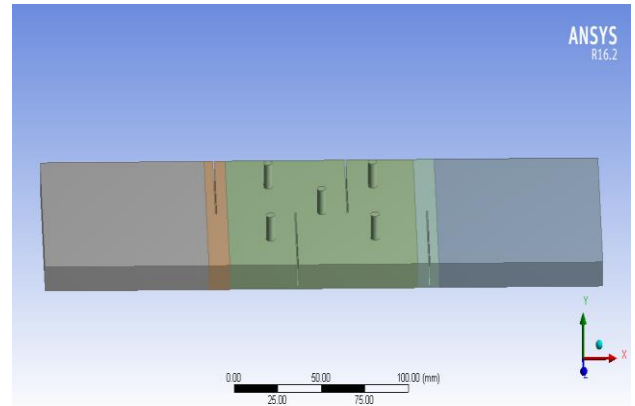


Fig-1: Geometry of the model

### 2.2 Governing equations

Numerical simulation of the flow and thermal fields in the computational domain requires solving the continuity (1), momentum (2) and energy (3) conservation equations which are expressed as follows:

$$\frac{\partial u_i}{\partial x_i} = 0 \tag{1}$$

$$\rho \frac{\partial u_i}{\partial t} + \rho \frac{\partial (u_i u_j)}{\partial x_j} = -\frac{\partial P}{\partial x_i} + \frac{\partial}{\partial x_j} \left[ \mu \left( \frac{\partial u_i}{\partial x_j} + \frac{\partial u_j}{\partial x_i} \right) - \rho \overline{u_i u_j} \right] + \rho g_i \tag{2}$$

$$\rho c_p \left[ \frac{\partial T}{\partial t} + \frac{\partial (u_i T)}{\partial x_i} \right] = \frac{\partial}{\partial x_i} \left( k \frac{\partial T}{\partial x_i} - \rho c_p \overline{u_i T'} \right) \tag{3}$$

Here there are Reynolds stress tensor and turbulence heat flux vector, respectively, which need to be modeled with a suitable turbulence model. The turbulence model took was SST  $k-\omega$  model.

The SST  $k-\omega$  turbulence model is a two-equation eddy-viscosity model which has become very popular. The shear stress transport (SST) formulation combines the best of two worlds. The use of a  $k-\omega$  formulation in the inner parts of the boundary layer makes the model directly usable all the way down to the wall through the viscous sub-layer, hence the SST  $k-\omega$  model can be used as a Low-Re turbulence model without any extra damping functions. The SST formulation also switches to a  $k-\epsilon$  behavior in the free-stream and thereby avoids the common  $k-\omega$  problem that the model is too sensitive to the inlet free-stream turbulence properties. Authors who use the SST  $k-\omega$  model often merit it for its good behavior in adverse pressure gradients and separating flow. The SST  $k-\omega$  model does produce a bit too large turbulence levels in regions with large normal strain, like stagnation regions and regions with strong acceleration. This tendency is

much less pronounced than with a normal k-ε model though.

The governing equations for SST k- ω model is as follows:

Kinematic Eddy viscosity,

$$\nu_T = \frac{a_1 k}{\max(a_1 \omega, SF_2)} \quad (4)$$

Turbulent Kinetic energy,

$$\frac{\partial k}{\partial t} + U_j \frac{\partial k}{\partial x_j} = P_k - \beta^* k \omega + \frac{\partial}{\partial x_j} \left[ (\nu + \sigma_k \nu_T) \frac{\partial k}{\partial x_j} \right] \quad (5)$$

Specific Dissipation rate,

$$\frac{\partial \omega}{\partial t} + U_j \frac{\partial \omega}{\partial x_j} = \alpha S^2 - \beta \omega^2 + \frac{\partial}{\partial x_j} \left[ (\nu + \sigma_\omega \nu_T) \frac{\partial \omega}{\partial x_j} \right] + 2(1 - F_1) \sigma_{\omega 2} \frac{1}{\omega} \frac{\partial k}{\partial x_i} \frac{\partial \omega}{\partial x_i} \quad (6)$$

Closure Coefficients and Auxiliary Relations,

$$F_2 = \tanh \left[ \max \left( \frac{2\sqrt{k}}{\beta^* \omega y}, \frac{500\nu}{y^2 \omega} \right) \right]$$

$$P_k = \min \left( \tau_{ij} \frac{\partial U_i}{\partial x_j}, 10\beta^* k \omega \right)$$

$$F_1 = \tanh \left\{ \min \left[ \max \left( \frac{\sqrt{k}}{\beta^* \omega y}, \frac{500\nu}{y^2 \omega} \right), \frac{4\sigma_{\omega 2} k}{CD_{kw} y^2} \right] \right\}^4$$

$$CD_{kw} = \max \left( 2\rho \sigma_{\omega 2} \frac{1}{\omega} \frac{\partial k}{\partial x_i} \frac{\partial \omega}{\partial x_i}, 10^{-10} \right)$$

$$\phi = \phi_1 F_1 + \phi_2 (1 - F_1)$$

$$\alpha_1 = \frac{5}{9}, \alpha_2 = 0.44$$

$$\beta_1 = \frac{3}{40}, \beta_2 = 0.0828$$

$$\beta^* = \frac{9}{100}$$

$$\sigma_{k1} = 0.85, \sigma_{k2} = 1$$

$$\sigma_{\omega 1} = 0.5, \sigma_{\omega 2} = 0.856$$

### 3. PROBLEM'S OBJECTIVE

#### 3.1 Problem statement

According to Fig.1, the problem of the present study consists of a three-dimensional geometry including multiple submerged impinging jets along with cross flow. In this study the main focus is given to the problem which

is to compare the heat transfer characteristics for different cross flow velocities and at the same time varying the gap between baffle and plate surface.

**Table -1: Input Parameters with respected ranges**

| Parameter  | Value Ranges      |
|--|-------------------|
| Nozzle diameter (D)  | 5mm               |
| Height between Nozzle to the Target plate (H)                                | 5mm               |
| Height between Nozzle to the Target plate to nozzle diameter (H/D)           | 1 (constant)      |
| Heat input to the plate  | 50watts           |
| Frequency (pulsations) (f)   | 40Hz (constant)   |
| Nozzle velocity  | 20 m/s (constant) |
| Blow ratio = $\frac{\text{cross flow velocity}}{\text{nozzle velocity}}$ (B) | 2,1.6,1.33,1      |
| Height of baffles  | 9mm,8mm,7mm       |

Following are the input factors which will be varying for the respective ranges. The heat input, nozzle velocity and the frequency of pulsation is kept throughout the analysis. The blow ratio (B) is varied by varying the cross flow velocity. For every case there will be a results providing the Nusselt Number (Nu) for them.

**Table -2: Properties of Air at 300K**

| Parameter                       | Value                    |
|---------------------------------|--------------------------|
| Specific Heat (C <sub>p</sub> ) | 1.0049 KJ/KgK            |
| Specific Heat (C <sub>v</sub> ) | 0.7178 KJ/KgK            |
| Dynamic Viscosity (μ)           | 1.846 x 10 <sup>-5</sup> |
| Thermal Conductivity (k)        | 0.02624 w/mK             |
| Prandtl Number (Pr)             | 0.707                    |
| Density (ρ)                     | 1.177 Kg/m3              |

Following are the properties which were included in the computational software ANSYS 16.2[16] before starting the computation for dry air at 300K (Temperature). Along with that some other basic parameters were also included in the software which didn't change themselves throughout all the computational cases.

#### 3.2 Experiment cases

By varying the different parameters total 12 cases were studied for the analysis.

**Table -3: Total Amount of Cases**

| No. | Baffle length (mm) | Blow ratio (B) |
|-----|--------------------|----------------|
| 1   | 9                  | 2              |
| 2   | 9                  | 1.6            |
| 3   | 9                  | 1.33           |
| 4   | 9                  | 1              |
| 5   | 8                  | 2              |
| 6   | 8                  | 1.6            |
| 7   | 8                  | 1.33           |
| 8   | 8                  | 1              |
| 9   | 7                  | 2              |
| 10  | 7                  | 1.6            |
| 11  | 7                  | 1.33           |
| 12  | 7                  | 1              |

**4. FLUENT SIMULATION**

All governing equations were solved by the control volume approach using commercial software ANSYS Fluent 16.2. The double precision option was adopted for all computations, since it will include all the 6 digit significant values to the answer. The velocity components are evaluated at the control volume faces, while the rest of the variables governing the flow field are stored at the central node of the control volume. The flow and thermal fields was computed with the finite volume computational fluid dynamics (CFD) code FLUENT. In pulsed turbulent impinging jets, turbulence components are highly anisotropic due to strong compression of turbulence, chaotic mixing and nonlinear dynamic response of boundary layers. The SST k- ω turbulence model is numerically robust and fast, and has been proven to be effective in modelling this type of complex flows in impinging and opposed jets.

**4.1 Model Validation**

The numerical results obtained by present study were compared with the experimental results of Mladin (7) The experimental apparatus was set up at Reynolds Number 5500 for a frequency of 41 Hz at H/D = 5. Numerical results were in good agreement with the experiment results. Mladin carried out experiment on local convective heat transfer to submerged pulsating jets. Figure 2 shows the graph between Nusselt Number and plate distance for both cases.

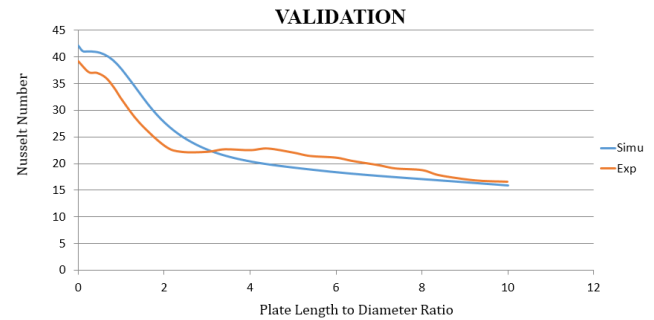


**Fig -2: Validation Curve**

From the graph as we can see that there is an overall average deviation of 8.6% with maximum deviation occurring just after 0 on radial distance for 15.1%.

**5. RESULTS AND DISCUSSION**

Firstly a case was run for 3 seconds by taking results in each 0.3 seconds. It was found that after first 0.3 seconds the results were consistent. So all the other cases were run for 0.3 seconds only. The values of average Nusselt number and surface temperature are shown in table-4.

The lowest temperature was attained for the case with baffle length 9mm and blow ratio 2. For all the baffle length the maximum Nusselt number and heat transfer characteristics was got at blow ratio 2.

**Table-4: Average values of surface Nusselt number and average surface temperature after simulation**

| Baffle length | Blow ratio | Average values of static temperature in heating plate (K) | Average values of Surface Nusselt Number on plate surface |
|---------------|------------|---|---|
| 9mm           | 2          | 306.569   | 119.791   |
|               | 1.6        | 307.866   | 99.0615   |
|               | 1.33       | 309.03  | 87.5635   |
|               | 1          | 311.263   | 68.9915   |
| 8mm           | 2          | 307.599   | 97.967  |
|               | 1.6        | 309.066   | 81.836  |
|               | 1.33       | 310.449   | 70.8325   |
|               | 1          | 312.504   | 60.025  |
| 7mm           | 2          | 308.735   | 82.345  |
|               | 1.6        | 310.932   | 66.6975   |
|               | 1.33       | 312.607   | 57.838  |
|               | 1          | 315.606   | 46.47255  |

### 5.1 Variation in Nusselt number

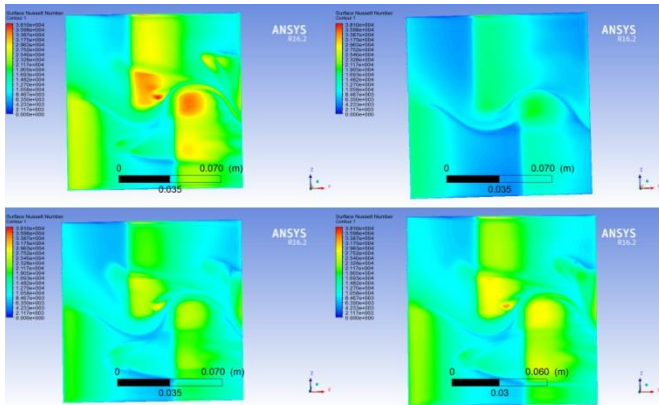


Fig.2 Nusselt number contour for baffle length 9mm

Fig.2 shows the Nusselt number contour for all the 4 cases for baffle length 9mm. The first contour shows for blow ratios 1. Here we can see that air enters through left side and hits the second baffle and generates turbulence. We can see that the maximum Nusselt number is between the second and third baffle. Here there is maximum effect of both cross flow and pulsating flow from nozzle. It is because of the turbulence created by the cross flow after hitting the second baffle.

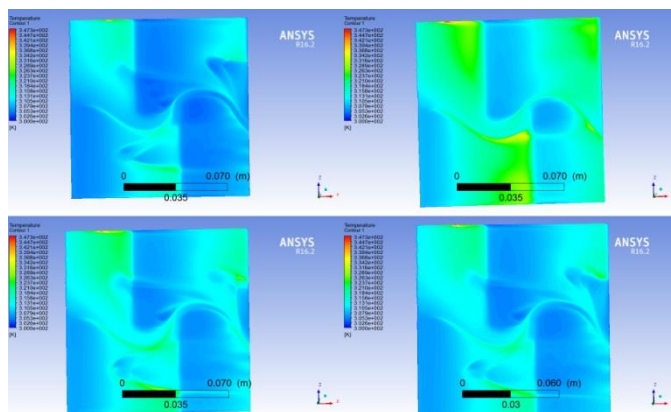


Fig.3 Temperature contour for baffle length 9mm

The temperature contour in fig 3 also shows the same trending pattern as same as the Nusselt number contour. Similar patterns are shown for baffle length 8mm and 7mm. Average surface temperature and surface Nusselt number values were taken to analyze the heat transfer characteristics

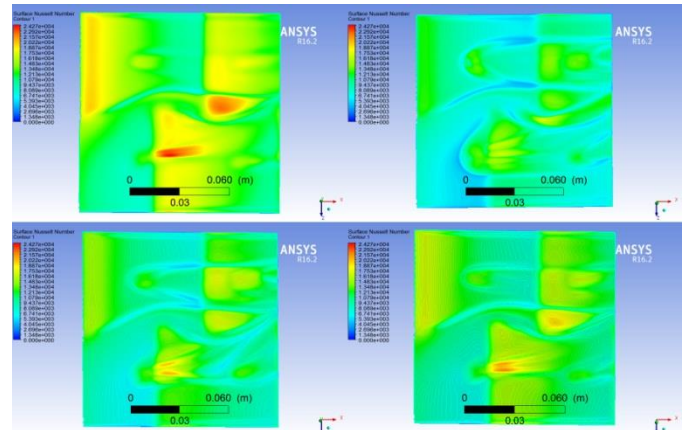


Fig-4 : Nusselt number contour for baffle length 8mm

Although the average Nusselt number is lower for case with baffle length 8mm (fig-4) than baffle length 9mm (fig-3), the Nusselt number contour is more uniformly distributed in this case. As the gap between the baffle and plate is 2m, more fluid from cross flow interacts between the flows from the nozzle and creates turbulence more uniformly.

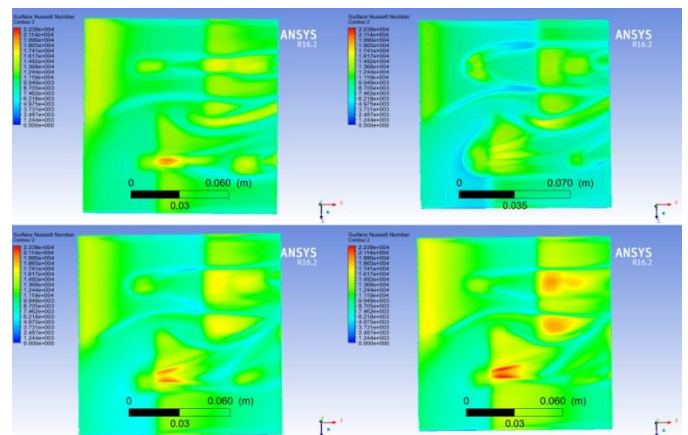


Fig-5 : Nusselt number contour for baffle length 7mm

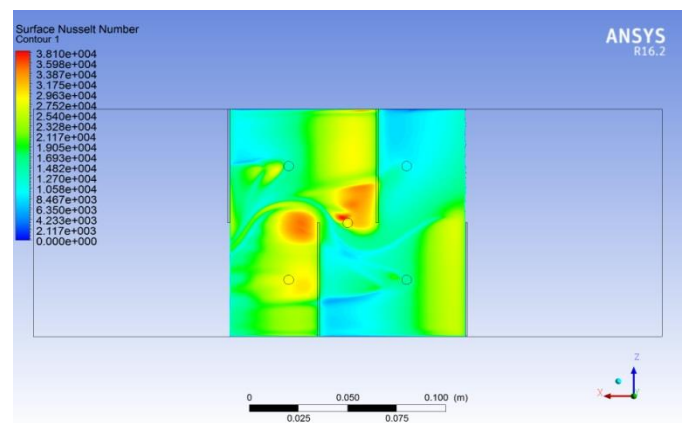


Fig-6 : Nusselt number contour for baffle length 9mm and blow ratio 2

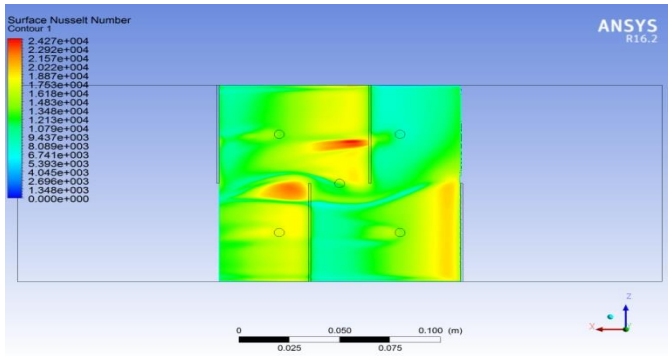


Fig-7 : Nusselt number contour for baffle length 8mm and blow ratio 2

For baffle with 7mm length (fig-5), it shows the least Nusselt number characteristics. As the gap becomes 3 mm the cross flow swipes away the flow from the nozzles completely thus reducing the turbulence.

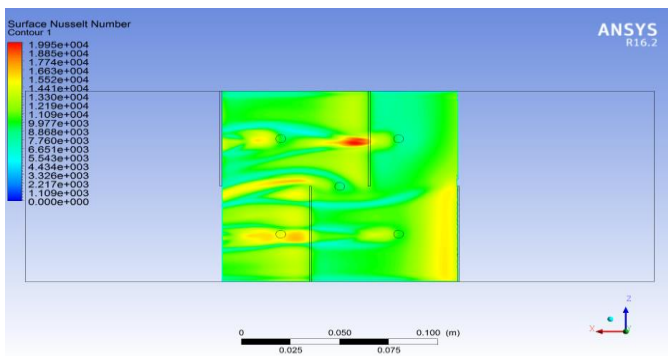


Fig-8 : Nusselt number contour for baffle length 7mm and blow ratio 2

For all baffle lengths, the blow ratio 2 showed the maximum Nusselt number characteristics (fig-6,7,8) which reflects the heat transfer characteristics.

A line was drawn diagonally through the region which showed maximum heat transfer characteristics and Nusselt number values across that line (fig-9).

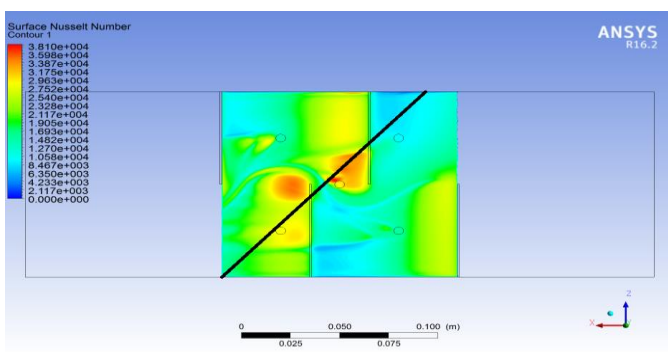


Fig-9 :line drawn on the contour through the region which showed maximum uniformity in Nusselt number

Nusselt number was plotted across that line and the result is shown in fig-10. Flow is from left to right. As the cross flow approaches from left we can see that the Nusselt number increases as vorticity and turbulence increases. Finally when the cross flow exits, the velocity gets decayed and thus reducing the heat transfer characteristics. Maximum Nusselt number is in the middle region between the second and third baffle (fig-10).

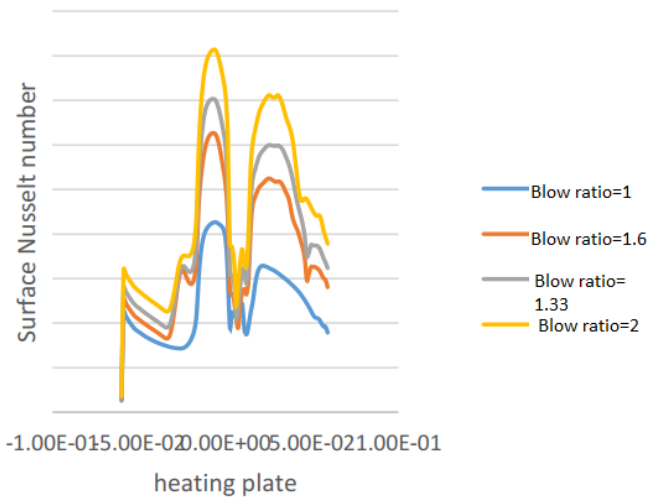


Fig-10: Variation of Nusselt number along the line in fig-9

### CONCLUSION

The present analysis was done to study the effect of pulsation along with the jet impingement heat transfer with cross flow. For all baffle lengths, the blow ratio 2 demonstrated the most extreme Nusselt number characteristics (fig-6,7,8). From the averaged data it is concluded that as the blow ratio decreases the heat transfer characteristics also decreases. But we cannot increase blow ratio beyond a particular value as increase in blow ratio increases the air mass flow rate beyond a limit. Also in all cases the baffle with 1mm gap came with extreme Nusselt number characteristic and average surface temperature. As the baffle length increases it swipes away all the flow from nozzles and reduces the region of turbulence and vorticity effects which is directly proportional to heat transfer.

### REFERENCES

- [1] Womac D and Incropera. "Single Phase Liquid Jet Impingement Cooling of Small Heat Sources", International Heat Transfer Conference, 1990
- [2] Dushyant Singh, B. Premachandran. "Experimental and numerical investigation of jet impingement

cooling of a circular cylinder”,International Journal For Heat And Mas Transfer 2013,IIT Delhi.

- [3] Jung -Yang San.”Optimum jet to jet spacing for heat transfer in staggered array”,International Journal For Heat And Mass Transfer,2001,at Taiwan K. Elissa.
- [4] R. Zulkifli, K. Sopian,”Studies On Pulse Jet Impingement Heat Transfer: Flow Profile And Effect Of Pulse Frequencies On Heat Transfer”, International Journal of Engineering and Technology 2007,Malaysia.
- [5] M.Angioletti,”CFD turbulent modelling of jet impingement and its validation by particle image velocimetry and mass transfer measurements”, International Journal of Thermal Sciences 44 (2005) 349-356,2004
- [6] Gorka S. Larraona ,“Computational parametric study of an impinging jet in a cross-flow configuration for electronics cooling applications”,\_Applied Thermal Engineering 52 (2013)
- [7] E. C. Mladin, D. A. Zumbrunnen (1996), “Local Convective heat transfer to submerged pulsating jets”, International Journal of Heat and Mass Transfer, Vol. 40, pp. 3305-3321.